Crystal Structure of NADH−Cytochrome b_5 Reductase from Pig Liver at 2.4 Å Resolution[†,‡]

Hirokazu Nishida,[§] Koji Inaka,[§] Masaki Yamanaka,[∥] Satoshi Kaida,[∥] Kazuo Kobayashi,[⊥] and Kunio Miki*[,§]

Research Laboratory of Resources Utilization, Tokyo Institute of Technology, Nagatsuta, Midori-ku, Yokohama 227, Japan, Department of Applied Chemistry, Faculty of Engineering, Osaka University, Yamadaoka, Suita, Osaka 565, Japan, and Institute of Scientific and Industrial Research, Osaka University, Mihogaoka, Ibaraki, Osaka 567, Japan

Received August 18, 1994; Revised Manuscript Received December 8, 1994[⊗]

ABSTRACT: The three-dimensional structure of NADH−cytochrome b_5 reductase from pig liver microsomes has been determined at 2.4 Å resolution by X-ray crystallography. The molecular structure reveals two domains, the FAD binding domain and the NADH domain. A large cleft lies between these two domains and contains the binding site for the FAD prosthetic group. The backbone structure of the FAD binding domain has a great similarity to that of ferredoxin−$NADP^+$ reductase [Karplus, P. A., Daniels, M. J., & Herriott, J. R. (1991) *Science 251,* 60−65], in spite of the relatively low sequence homology (about 15%) between the two enzymes. On the other hand, the structure of the NADH domain has several structural differences from that of the $NADP^+$ domain of ferredoxin−$NADP^+$ reductase. The size of the cleft between the two domains is larger in NADH−cytochrome b_5 reductase than in ferredoxin−$NADP^+$ reductase, which may be responsible for the observed difference in the nucleotide accessibility in the two enzymes.

Fatty acids are physiologically important both as components of phospholipids and glycolipids and as fuel molecules. In fatty acid synthesis, the major product of the fatty acid synthase is palmitate. Longer fatty acids are formed by elongation reactions catalyzed by enzymes located on the endoplasmic reticulum membrane, in which double bonds are also introduced into long-chain acyl coenzymes A. For example, stearoyl coenzyme A is converted into oleoyl coenzyme A by an oxidase using molecular oxygen and NADH. This desaturation reaction is catalyzed by a complex of three membrane-bound enzymes: NADH−cytochrome b_5 reductase (b5R,[1] EC 1.6.2.2), cytochrome b_5, and a desaturase (Keyes & Cinti, 1980; Oshino et al., 1971). In the endoplasmic reticulum of liver microsomes, b5R catalyzes the two-electron transfer from NADH to cytochrome b_5 through the enzyme-bound FAD molecule (Strittmatter, 1965; Iyanagi, 1977). The enzyme purified from liver microsomes is an amphipathic membrane-bound flavoprotein containing a large (31 kDa) hydrophilic, catalytic domain and a smaller (3 kDa) hydrophobic membrane-binding segment (Spatz & Strittmatter, 1973). The b5R from pig liver microsomes can be purified in the following two ways: the intact form of the protein molecule can be solubilized by the use of detergents (detergent-solubilized enzyme), or the hydrophilic, catalytic domain can be obtained by the removal of the membrane-binding fragment using cathepsin D from lysosome (lysosome-solubilized enzyme). Both forms of the enzyme were crystallized. The latter form gave crystals suitable for high-resolution X-ray crystallography (Miki et al., 1987). The soluble form of this enzyme from human erythrocytes was also crystallized in a different crystal system (Takano et al., 1987).

The three-dimensional structure of b5R gives important information for understanding the mechanism of electron transfer from NADH to a complex of three membrane-bound enzymes. We report here the crystal structure of the lysosome-solubilized form of pig liver b5R determined at 2.4 Å resolution by X-ray crystallography.

MATERIALS AND METHODS

The lysosome-solubilized hydrophilic domain of b5R was purified from pig liver microsomes (Iyanagi et al., 1984) and crystallized as described previously (Miki et al., 1987). The crystals belong to the space group $P2_12_12_1$ with unit cell dimensions of a = 86.9 Å, b = 73.1 Å, and c = 48.9 Å (Miki et al., 1987). The crystal structure was initially solved by multiple isomorphous replacement (MIR) using diffraction data at 2.5 Å resolution collected on six different heavy-atom derivatives (Table 1). Derivatives were prepared by soaking in solutions of heavy-metal compounds (1−10 mM) for 1−2 days. Diffraction data were mainly collected on a DIP100s rotation camera system equipped with an imaging plate (Mac Science Co. Ltd., Tokyo, Japan) and evaluated using the program ELMS (Tanaka et al., 1990), while Sakabe's Weissenberg method was partly employed for the purpose of the derivative search with synchrotron radiation at the Photon Factory, National Laboratory for High Energy

[†] This work is supported in part by Grants-in-Aid for Scientific Research from the Ministry of Education, Science and Culture, Japan, to K.M., and by CIBA-GEIGY Foundation (Japan) for the Promotion of Science to K.M.

[‡] Coordinates for the crystal structure of NADH−cytochrome b_5 reductase have been deposited with the Brookhaven Protein Data Bank under the file name 1NDH.

* To whom correspondence should be addressed at the Department of Chemistry, Faculty of Science, Kyoto University, Sakyo-ku, Kyoto 606-01, Japan.

[§] Tokyo Institute of Technology.

[∥] Faculty of Engineering, Osaka University.

[⊥] Institute of Scientific and Industrial Research, Osaka University.

[⊗] Abstract published in *Advance ACS Abstracts,* February 1, 1995.

[1] Abbreviations: NADH, nicotinamide adenine dinucleotide; FAD, flavin adenine dinucleotide; b5R, NADH−cytochrome b_5 reductase; FNR, ferredoxin−$NADP^+$ reductase; PDR, phthalate dioxygenase reductase.

0006-2960/95/0434-2763$09.00/0

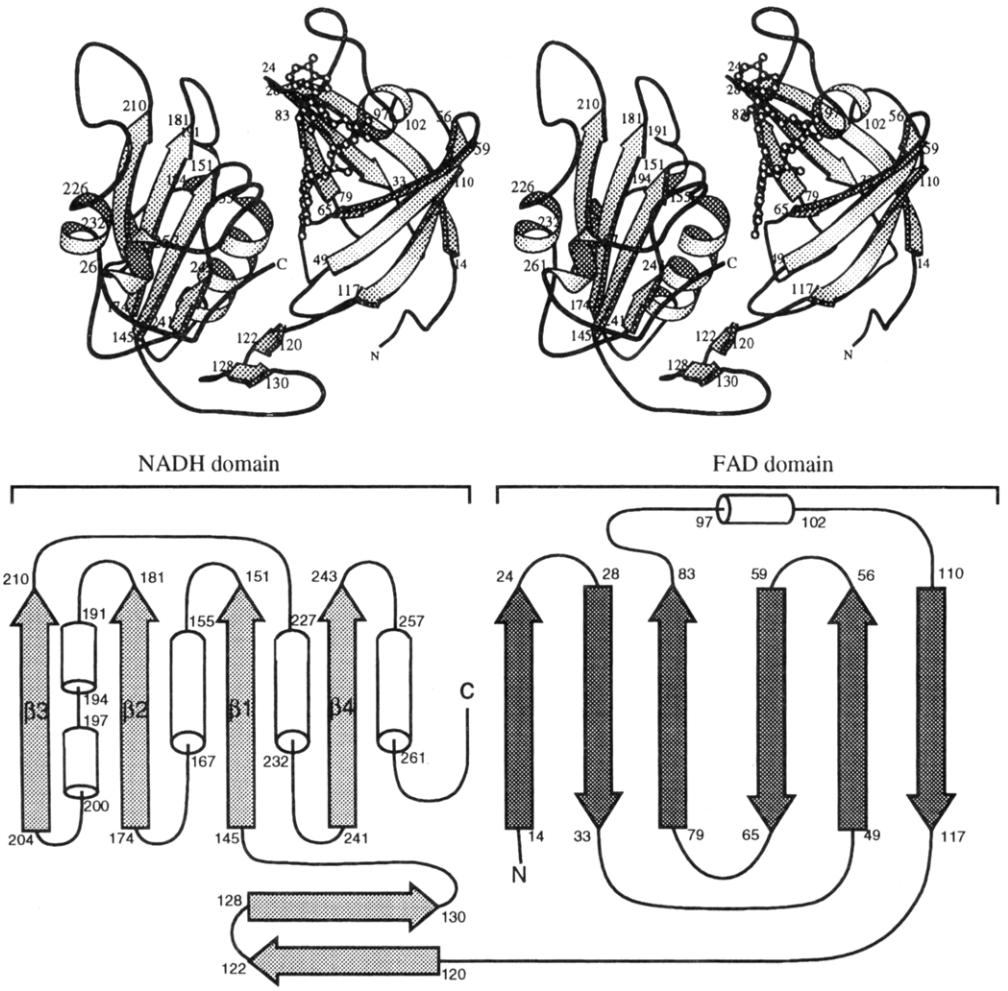

FIGURE 1: (a, top) Stereo diagram of the b5R molecule generated using the program MOLSCRIPT (Kraulis, 1991). The FAD prosthetic group is represented by the ball and stick model. Numbers denote the residue number. The molecule is divided into two domains, NADH (left) and FAD (right) domains, by a large cleft in which the FAD molecule is located. (b, bottom) Schematic drawing of the secondary structure. α-Helices are shown as cylinders and β-strands as arrows. A short two-stranded β-sheet at the N-terminus of the NADH domain connects the two domains.

Table 1: Diffraction Data (∞−2.0 Å) and Phasing Statistics (15.0−2.5 Å)

data set	unique reflections	R_{merge}[a] (%)	R_{iso}[b] (%)	no. of sites	phasing power[c]
native	18 695	5.5			
$KAu(CN)_2$	16 084	5.5	20.5	1	2.16
$C_9H_9HgO_2SNa$	17 556	5.7	17.9	3	2.60
CH_3HgCl	18 080	10.4	28.6	3	2.54
t-$PtCl_2(NH_3)_2$	16 599	7.6	18.6	1	0.49
$TbCl_3$	17 622	7.1	13.2	2	1.09
$IrCl_4$	17 451	6.8	14.3	2	1.06

[a] $R_{merge} = \sum|I_i - I_{av}|/\sum I_{av}$, where I_i and I_{av} are individual and average intensities of measurements, respectively. [b] $R_{iso} = \sum|F_{native} - F_{derivative}|/\sum F_{native}$, where F_{native} and $F_{derivative}$ are the native and derivative structure factors, respectively. [c] Phasing power is defined as the mean value of the heavy-atom structure factor amplitude divided by the residual lack of closure error. The *t*-$PtCl_2(NH_3)_2$ derivative with low phasing power is not excluded because it made a contribution to phasing at low resolution.

Physics, Tsukuba (Sakabe, 1991). Further crystallographic calculations were performed with the program package PROTEIN (Steigemann, 1992). The electron density map at 2.5 Å resolution based on refined heavy-atom parameters had a mean figure of merit of 0.75 but was not enough to trace the polypeptide chain completely. The solvent flattening technique (Wang, 1985) improved the electron density map with a mean figure of merit of 0.85, which allowed construction of 80% of the whole molecule. The structural model was constructed on an Evans & Sutherland PS390 graphics system with the program FRODO (Jones, 1978). The complete amino acid sequence of b5R from pig liver has not yet been determined. About 60% of the whole sequence is at present available (Crabb et al., 1980; Iyanagi, personal communication; Nakane and Matsui, personal communication). The amino acid sequence of b5R from steer liver microsomes (Ozols et al., 1985) was employed for the unknown region of pig liver b5R, because the sequence identity in the available region between these two enzymes is more than 90%. Subsequently, maps were calculated with the MIR phases merged with the partial model phases by Sim's weighting scheme. After three cycles of model building and phase combination, the complete molecular model could be constructed including the bound FAD molecule. The model was refined by the simulated-annealing method using the program X-PLOR at 2.4 Å resolution (Brünger et al., 1990). Afterward, stereochemically restrained least-squares refinement was performed with native data from 5.0 to 2.4 Å resolution using the program package PROLSQ (Hendrickson, 1985). The present model containing 2158 atoms of the protein molecule and 53 atoms of the prosthetic group, FAD, has a crystallographic *R* value

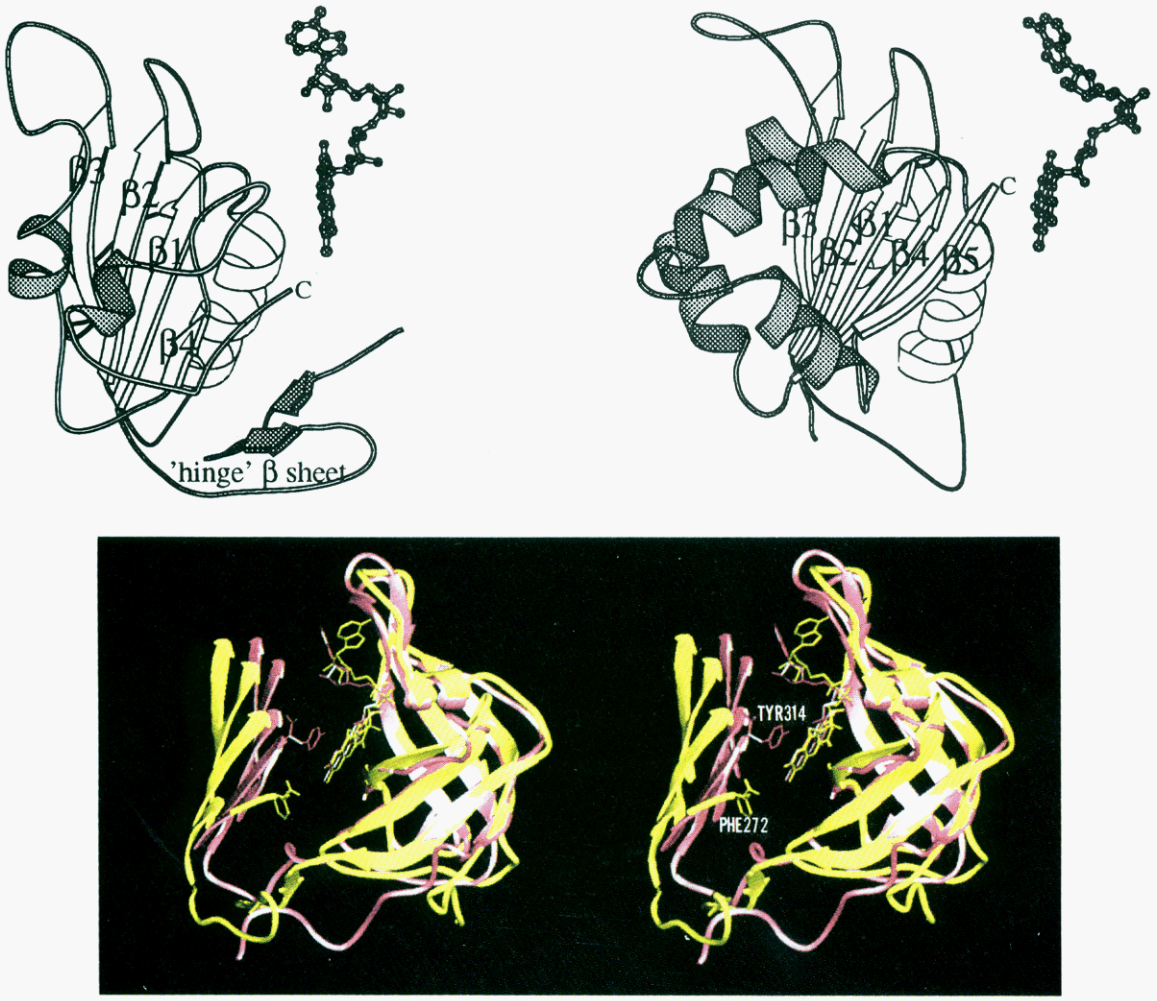

FIGURE 2: (a, top) Schematic diagrams (Kraulis, 1991) of the NADH domain in b5R (left) and the NADPH domain in FNR (right). Shaded regions indicate structural differences between the two structures described in the text. (b, bottom) Schematic diagrams of the FAD domains and the large parallel β-sheets of the NAD(P)H domains in b5R (yellow) and FNR (red) generated using the program RIBBON (Carson, 1987). The FAD molecules and the last residues, Phe272 of b5R and Tyr314 of FNR, are represented by the stick model. Both structures are superimposed as follows: each isoalloxazine ring of the FAD is manually adjusted at first, and then residue pairs nearby each other between b5R and FNR in FAD domains are assigned. The transformation matrix for the FAD domain of FNR is calculated by minimizing the rms distances between Cα atoms of the assigned residue pairs. It is shown in this figure that the configurations of β-sheets in NADH (NADPH) domains are clearly different against each FAD domain. The side chain of the last residue in b5R (Phe272) is away from the isoalloxazine ring of FAD while that in FNR (Tyr314) is stacked to the ring (see text).

of 23.7% for all 10 350 reflections between 5.0 and 2.4 Å resolution. The average rms deviation from the standard bond length is 0.016 Å.

RESULTS AND DISCUSSION

The molecular model includes the FAD prosthetic group and the protein chain from residue 3 through the carboxyl terminus at residue 272. The most striking feature of the structure is that the molecule is composed of two domains, the FAD binding domain and the NADH domain (Figure 1). The approximate overall dimensions are 40 × 50 × 55 Å. The first domain, residues 3 through 118, that binds the FAD prosthetic group consists of an antiparallel β-barrel core and a single α-helix. The barrel core consists of two of the three-stranded antiparallel β-sheets. The top of this barrel is capped by an α-helix and a loop region which binds the adenine portion of FAD. This adenine binding loop region curves around the framework of the adenine portion. The second domain, residues 119 through 272, has a central four-stranded parallel β-sheet, five surrounding helices, and a two-stranded antiparallel β-sheet which is located at the N-terminus of this domain near the FAD domain. This small antiparallel β-sheet behind a large cleft appears to determine the relative position of the two domains. Similar topology to the FAD and NADH domains of b5R is also observed in ferredoxin−$NADP^+$ reductase (FNR) (Karplus et al., 1991) and phthalate dioxygenase reductase (PDR) (Correll et al., 1992), although the latter contains an additional 2Fe-2S domain. The structural homology between b5R and FNR was predicted from the primary sequence analysis (Karplus et al., 1991; Hyde et al., 1991). The structural comparison is hereafter carried out mainly using the FNR structure. When the two FAD domain structures of b5R and FNR are superimposed, about 77% of the Cα atoms are within 2.0 Å of their equivalent atomic positions. In the case of the NAD(P)H domain, about 48% of the Cα atoms in b5R are located within 2.0 Å from those in FNR. On the other hand, the structural motif of the NADH domain is the so-called Rossmann fold widely observed in not only b5R and FNR but also the other nucleotide binding proteins, such as lactate dehydrogenase, glutathione reductase, glyceraldehyde-phosphate dehydrogenase, and alcohol dehydrogenase (Rossmann et al., 1974).

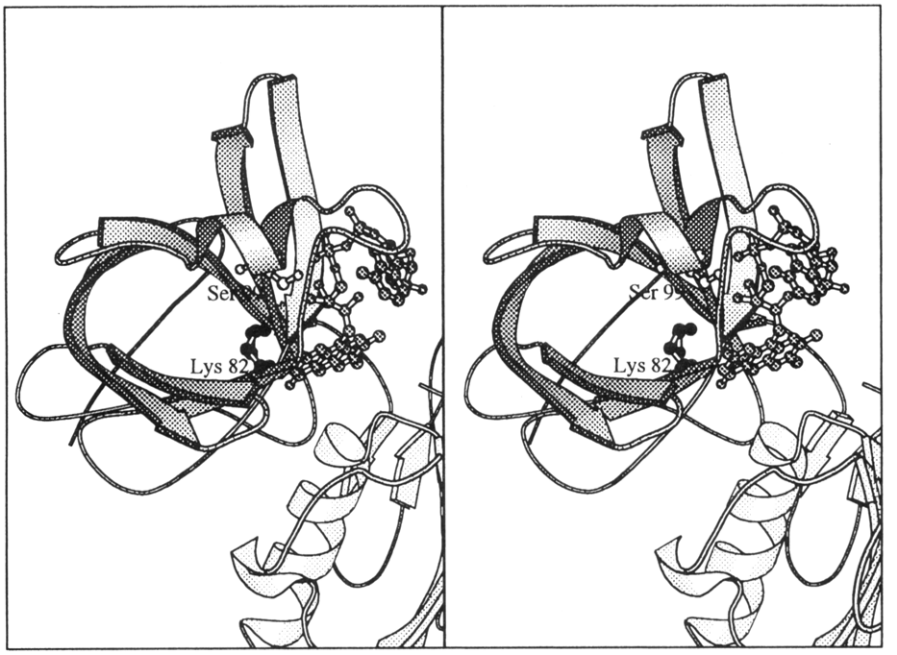

FIGURE 3: Stereo diagram around the FAD binding site in b5R. Lys82 (black ball), Ser99 (white), and FAD (gray) are represented by the ball and stick model. Both Lys82 and Ser99 contact with the FAD molecule located inside of the barrel of the FAD domain and have no direct interaction with residues in the NADH domain.

There are two remarkable structural differences between b5R and FNR. First, the two-stranded antiparallel β-sheet at the N-terminus of the NADH domain (residues 120 through 130) plays a hinge-connecting role between two domains and seems to determine the width of the cleft; the cleft of b5R is larger than that of FNR. This β-sheet structure is not observed in FNR (Figure 2a). Second, the interaction of the C-terminal last residues with FAD in b5R is different from FNR. The positions of these C-terminal last residues depend on the width of the cleft. The side chain of the C-terminal Phe272 of b5R is more than 6 Å apart from the FAD, while the C-terminal Tyr314 of FNR is stacked against the isoalloxazine plane of FAD (Figure 2b). Phe272 is included in the region where the amino acid sequence from pig liver b5R is known, and its side chain is clearly assigned in the electron density map.

In addition to these two, some other structural differences can be pointed out. The loop region in b5R which binds the adenine portion of FAD has a different structure from that in FNR, resulting in an alternate conformation of the adenine portion of FAD in these two proteins (Figure 2b). There is a short antiparallel β-sheet in this region of FNR. This conformational change is partly due to the crystal packing effect because the closest interatomic contacts between adjacent molecules are about 3 Å in this region. On the other hand, a single α-helix exists between strands β3 and β4 of the NADH domain of b5R, while two helices are located in this region of FNR, although the number of residues involved between β3 and β4 in b5R (30 residues) is comparable with that in FNR (33 residues) (Figure 2a). In addition, only one α-helix is located after the β4 strand at the C-terminal region of b5R, while two helices and one β-strand are existent at the corresponding region of FNR.

The hinge β-sheet at the N-terminus of the NADH domain in b5R mentioned above seems to induce a slight rotation of the NADH domain from the corresponding position in FNR. Consequently, the cleft between the two domains in b5R is widened. The larger cleft in b5R results in fewer atomic contacts between the two domains than those in FNR. The interface areas between the two domains are 1550 Å^2 for b5R and 2800 Å^2 for FNR (Kabsch et al., 1983), on the basis of the solvent-accessible surface. There are five hydrogen bonds at the interface between the NADH and FAD domains in b5R, whereas 13 hydrogen bonds are formed between the two domains in FNR. As shown in Figure 2b, the parallel β-sheet in the NADH domain of b5R is displaced further away from the FAD domain compared with that in the NADP$^+$ domain of FNR. The relative orientation of this β-sheet and the FAD domain also differs in b5R and FNR. Consequently, Tyr314 of FNR (stick model in red in Figure 2b) is stacked against the isoalloxazine ring of FAD, whereas Phe272 of b5R (stick model in yellow) is kept away from this ring.

In the 2′-phospho-AMP binding structure of FNR, the distance from the AMP binding site to the FAD isoalloxazine ring and the direction of the bound AMP suggest that the nicotinamide moiety of NADP$^+$ may directly interact with the isoalloxazine ring (Karplus et al., 1991), and direct electron transfer between NADP$^+$ and the *re* side of isoalloxazine has been confirmed by ^{2}H-labeling experiments (Manstein et al., 1987). In the structure of NADPH binding glutathione reductase (Karplus et al., 1989), a Tyr residue is displaced by the nicotinamide moiety to form a complex in which the nicotinamide is stacked against the flavin ring. It is likely also in b5R that NADH approaches the FAD isoalloxazine ring with its nicotinamide ring at the head when the hydride transfer takes place and that the nicotinamide and isoalloxazine rings are finally stacked. The C-terminal Tyr314 of FNR is stacked against the FAD isoalloxazine ring and completely covers the N5 atom which provides a hydride ion to the nucleotide. In the case of b5R, the C-terminal Phe272 is located far from the isoalloxazine ring, and there is a considerable open space at the *re* side of the N5 atom in the FAD isoalloxazine ring. This open space may permit easy access of the nicotinamide of NADH to

the FAD isoalloxazine ring in b5R. This structural difference is consistent with the results from the kinetic experiments in b5R and FNR. The K_m value of the enzymatic reaction of b5R with NADH (0.4−0.5 μM) is about 100-fold smaller than that of FNR with $NADP^+$ (30 μM), and the comparison of K_d values obtained from experiments in the analogous states (oxidized b5R + NADH and reduced FNR + $NADP^+$) gave a much higher value of K_{on} of b5R than that of FNR (Batie & Kamin, 1984; Iyanagi et al., 1984).

The nucleotide accessibility is thought to be affected by various structural features. The NADH binding form of PDR shows that the NADH nicotinamide ring, the side chain of Phe225, and the isoalloxazine ring are stacked in triplicate to form a "gate-closed" state (Correll et al., 1992). The above Phe225 corresponds to the last residues (Phe272 and Tyr314) in b5R and FNR. These last residues, by which the *re* side of the FAD isoalloxazine ring is "gate opened" or gate closed, play an important role in adjusting the nucleotide accessibility for electron transfer between NAD(P)H and FAD. The b5R molecule seems to accept the NADH molecule without conformational change of the C-terminal region including Phe272, while in FNR, Tyr314 has to move out as observed in the electron-transfer reaction of glutathione reductase (Pai et al., 1988).

Several experiments modifying specific residues or mutations have been reported with this enzyme. Lys82 is suggested to be involved in binding to NADH by studies using site-directed mutagenesis and acetylation of lysine. The acetylation of this residue blocked the NADH binding to b5R (Hackett et al., 1988). Site-directed mutation of Lys82 to Gln or His showed a remarkable increase in the K_m values for NADH (Strittmatter et al., 1992). Figure 3 shows that Lys82 in the present structure is located behind the FAD isoalloxazine ring. The side chain of this residue is directed to the opposite side of FAD and toward the inside of the barrel without any hyddrogen bonds with FAD. On the other hand, it was predicted by the studies using Ser99Pro and Ser99Ala mutants of b5R from human erythrocytes that Ser99 plays an important role in maintaining the NADH binding site (Yubisui et al., 1991). Ser99 is conserved between pig and human b5R's. Site-directed mutation of this Ser to Pro or Ala results in a protein with altered spectral properties and a 10-fold higher K_m for NADH as compared with the wild type. In the present structure, Ser99 is positioned in the α-helix of the FAD domain with its side chain bound to the phosphate group of FAD (Figure 3). Both Lys82 and Ser99 residues may affect the binding ability of FAD, but they are not included in direct binding with NADH. The Ser99Pro mutation is known as hereditary methemoglobinemia type 2 (Yubisui et al., 1991). It is suggested by the present structure that mutation of Ser99 brings a significant conformational change in this α-helix and induces the enzymatic instability in b5R, because the Pro cyclic residue often breaks a formation of α-helix and the hydrophobic side chain is not hydrogen bonded to the FAD molecule.

NOTE ADDED IN PROOF

The crystal structure of the FAD-containing fragment of nitrate reductase, which is homologous with b5R, has been recently reported (Lu et al., 1994).

ACKNOWLEDGMENT

The authors thank Prof. T. Iyanagi for valuable discussions, Prof. N. Kasai for his support at the early stage of this study, and H. Nakane and T. Matsui for the partial amino acid sequence. They are also indebted to Drs. N. Sakabe and A. Nakagawa for their help in data collection with synchrotron radiation, which was performed under the approval of the Photon Factory Advisory Committee (Proposal No.91-203), the National Laboratory for High Energy Physics of Japan.

REFERENCES

Batie, C. J., & Kamin, H. (1984) *J. Biol. Chem. 259*, 11976−11985.
Brünger, A. T., Krukowski, A., & Erickson, J. W. (1990) *Acta Crystallogr. A46*, 585−593.
Carson, M. (1987) *J. Mol. Graphics 5*, 103−106.
Correll, C. C., Batie, C. J., Ballou, D. P., & Ludwig, M. L. (1992) *Science 258*, 1604−1610.
Crabb, J. W., Tarr, G. E., Yasunobu, K. T., Iyanagi, T., & Coon, M. J. (1980) *Biochem. Biophys. Res. Commun. 95*, 1650−1655.
Hackett, C. S., Novoa, W. B., Kensil, C. R., & Strittmatter, P. (1988) *J. Biol. Chem. 263*, 7539−7543.
Hendrickson, W. A. (1985) *Methods Enzymol. 115*, 252−270.
Hyde, G. E., Crawford, N. M., & Campbell, W. H. (1991) *J. Biol. Chem. 266*, 23542−23547.
Iyanagi, T. (1977) *Biochemistry 16*, 2725−2730.
Iyanagi, T., Watanabe, S., & Anan, K. F. (1984) *Biochemistry 23*, 1418−1425.
Jones, T. A. (1978) *J. Appl. Crystallogr. 21*, 273−288.
Kabsch, W., & Sander, C. (1983) *Biopolymers 22*, 2577−2637.
Karplus, P. A., & Schultz, G. E. (1989) *J. Mol. Biol. 210*, 163−180.
Karplus, P. A., Daniels, M. J., & Herriott, J. R. (1991) *Science 251*, 60−65.
Keyes, S. R., & Cinti, D. L. (1980) *J. Biol. Chem. 255*, 11357−11364.
Kraulis, P. J. (1991) *J. Appl. Crystallogr. 24*, 946−950.
Lu, G., Campbell, W. H., Schneider, G., & Lindqvist, Y. (1994) *Structure 2*, 809−821.
Manstein, D. J., Massey, V., & Pai, E. F. (1987) in *Flavins and Flavoproteins*, pp 3−12, Walter de Gruyter & Co., Berlin.
Miki, K., Kaida, S., Kasai, N., Iyanagi, T., Kobayashi, K., & Hayashi, K. (1987) *J. Biol. Chem. 262*, 11801−11802.
Oshino, N., Imai, Y., & Sato, R. (1971) *J. Biochem. 69*, 155−167.
Ozols, J., Korza, G., Heinemann, F. S., Hediger, M. A., & Strittmatter, P. (1985) *J. Biol. Chem. 260*, 11953−11961.
Pai, E. F., Karplus, P. A., & Schulz, G. E. (1988) *Biochemistry 27*, 4465−4474.
Rossmann, M. G., Moras, D., & Olsen, K. W. (1974) *Nature 250*, 194−199.
Sakabe, N. (1991) *Nucl. Instrum. Methods Phys. Res. A303*, 448−463.
Spatz, L., & Strittmatter, P. (1973) *J. Biol. Chem. 248*, 793−799.
Steigemann, W. (1992) *PROTEIN: A Program System for the Crystal Structure Analysis of Proteins*, Max-Planck-Institut für Biochemie, Martinsried, Germany.
Strittmatter, P. (1965) *J. Biol. Chem. 240*, 4481−4487.
Strittmatter, P., Kittler, J. M., & Coghill, J. E. (1992) *J. Biol. Chem. 267*, 20164−20167.
Takano, T., Ogawa, K., Sato, M., Bando, S., & Yubisui, T. (1987) *J. Mol. Biol. 195*, 749−750.
Tanaka, I., Yao, M., Suzuki, M., Hikichi, K., Matsumoto, T., Kozasa, M., & Katayama, C. (1990) *J. Appl. Crystallogr. 23*, 334−339.
Wang, B. C. (1985) *Methods Enzymol. 115*, 90−106.
Yubishi, T., Shirabe, K., Takeshita, M., Kobayashi, Y., Fukumaki, Y., Sakaki, Y., & Takano, T. (1991) *J. Biol. Chem. 266*, 66−70.

BI941910U